

THE MASSIVE AND DISTANT CLUSTERS OF *WISE* SURVEY :
MOO J1142+1527, A $10^{15} M_{\odot}$ GALAXY CLUSTER AT $Z = 1.19$

ANTHONY H. GONZALEZ¹, BANDON DECKER², MARK BRODWIN², PETER R. M. EISENHARDT³, DANIEL P. MARRONE⁴, S. A. STANFORD^{5,6}, DANIEL STERN³, DOMINIKA WYLEZALEK⁷, GREG ALDERING⁸, ZUBAIR ABDULLA^{9,10}, KYLE BOONE^{8,11}, JOHN CARLSTROM^{9,10}, PARKER FAGRELIUS^{8,11}, DANIEL P. GETTINGS¹, CHRISTOPHER H. GREER⁴, BRIAN HAYDEN^{8,12}, ERIK M. LEITCH^{9,10}, YEN-TING LIN¹³, ADAM B. MANTZ^{14,15}, STEPHEN MUCHOVEJ^{16,17}, SAUL PERLMUTTER^{8,11}, AND GREGORY R. ZEIMANN¹⁸

Submitted to The Astrophysical Journal Letters

ABSTRACT

We present confirmation of the cluster MOO J1142+1527, a massive galaxy cluster discovered as part of the Massive and Distant Clusters of *WISE* Survey. The cluster is confirmed to lie at $z = 1.19$, and using the Combined Array for Research in Millimeter-wave Astronomy we robustly detect the Sunyaev-Zel'dovich (SZ) decrement at 13.2σ . The SZ data imply a mass of $M_{200m} = (1.1 \pm 0.2) \times 10^{15} M_{\odot}$, making MOO J1142+1527 the most massive galaxy cluster known at $z > 1.15$ and the second most massive cluster known at $z > 1$. For a standard Λ CDM cosmology it is further expected to be one of the ~ 5 most massive clusters expected to exist at $z \geq 1.19$ over the entire sky. Our ongoing *Spitzer* program targeting ~ 1750 additional candidate clusters will identify comparably rich galaxy clusters over the full extragalactic sky.

Subject headings: galaxies: clusters: individual (MOO J1142+1527), clusters: intracluster medium

1. INTRODUCTION

In the past few years we have entered a new era of wide-area surveys capable of detecting galaxy clusters at $z > 1$. The previous generation of high-redshift cluster searches was the first to yield large samples of galaxy clusters at this epoch (e.g. Gladders & Yee 2005; Eisenhardt et al. 2008; Muzzin et al. 2009; Fassbender et al. 2011); however, these programs typically probed less than 100 deg^2 . Consequently, while these surveys have been effective in generating statistical sam-

ples of distant galaxy clusters, they have lacked the comoving volume to discover significant numbers of massive clusters ($M_{500c} \gtrsim 3 \times 10^{14} M_{\odot}$). The high mass tail of the galaxy cluster population is of significant interest for both galaxy evolution and cosmology. One open question is the extent to which the star formation, active galactic nuclei (AGN) activity, and assembly histories of cluster galaxies depend upon the mass of the cluster in which they reside (e.g. Brodwin et al. 2013; Ehlert et al. 2015; Ma et al. 2015). For this science, samples of high-mass clusters close to the epochs of assembly and star formation, coupled with existing lower mass samples, provide the necessary dynamical range to quantitatively address this question. For cosmology, massive, high-redshift clusters remain competitive probes of dark energy via a number of methods (e.g. Allen et al. 2011), including evolution in the cluster mass function (Vikhlinin et al. 2009; Bocquet et al. 2015), the clustering of galaxy clusters (e.g. Sereno et al. 2015), and through application of the f_{gas} test (Mantz et al. 2014). The high mass tail of the galaxy cluster mass function is also a sensitive indicator of primordial non-Gaussianity (Chen 2010; Williamson et al. 2011; Shandera et al. 2013).

In the last several years, the South Pole Telescope (SPT) and Atacama Cosmology Telescope (ACT) have each completed wide-area millimeter surveys to identify galaxy clusters via the Sunyaev-Zel'dovich effect, publishing cluster catalogs drawn from 2500 deg^2 for the SPT survey (Bleem et al. 2015) and 504 deg^2 for the ACT survey (Hasselfield et al. 2013). Together, these programs have published nearly 50 massive clusters at $z > 1$. The upcoming generation of optical, galaxy-based cluster searches will also extend into the wide-area, high-redshift region of parameter space, complementing these millimeter surveys. When complete, the Dark Energy Survey (Flaugher 2005; Sánchez & DES Collaboration 2010) is expected to result in a cluster catalog extending to $z \sim 1$, covering a $\sim 5000 \text{ deg}^2$ footprint that includes much of the SPT and ACT survey areas.

The Massive and Distant Clusters of *WISE* Survey (MaD-CoWS), which is designed to detect the most massive galaxy clusters at $z \approx 1$, offers the largest survey area among current

¹ Department of Astronomy, University of Florida, Gainesville, FL 32611-2055

² Department of Physics and Astronomy, University of Missouri, 5110 Rockhill Road, Kansas City, MO, 64110

³ Jet Propulsion Laboratory, California Institute of Technology, Pasadena, CA 91109

⁴ Steward Observatory, University of Arizona, Tucson, AZ 85121

⁵ Department of Physics, University of California, One Shields Avenue, Davis, CA 95616

⁶ Institute of Geophysics and Planetary Physics, Lawrence Livermore National Laboratory, Livermore, CA 94550

⁷ Department of Physics and Astronomy, Johns Hopkins University, Baltimore, MD 21218

⁸ Physics Division, Lawrence Berkeley National Laboratory, 1 Cyclotron Road, Berkeley, CA 94720

⁹ Department of Astronomy and Astrophysics, University of Chicago, Chicago, IL 60637

¹⁰ Kavli Institute for Cosmological Physics, University of Chicago, Chicago, IL 60637

¹¹ Department of Physics, University of California Berkeley, Berkeley, CA 94720

¹² Space Sciences Lab, University of California Berkeley, 7 Gauss Way, Berkeley, CA 94720

¹³ Institute of Astronomy and Astrophysics, Academia Sinica, Taipei, Taiwan

¹⁴ Kavli Institute for Particle Astrophysics and Cosmology, Stanford University, 452 Lomita Mall, Stanford, CA 94305

¹⁵ Department of Physics, Stanford University, 382 Via Pueblo Mall, Stanford, CA 94305

¹⁶ California Institute of Technology, Owens Valley Radio Observatory, Big Pine, CA 93513

¹⁷ California Institute of Technology, Department of Astronomy, Pasadena, CA 91125

¹⁸ Department of Astronomy and Astrophysics, Pennsylvania State University, University Park, Pennsylvania 16802

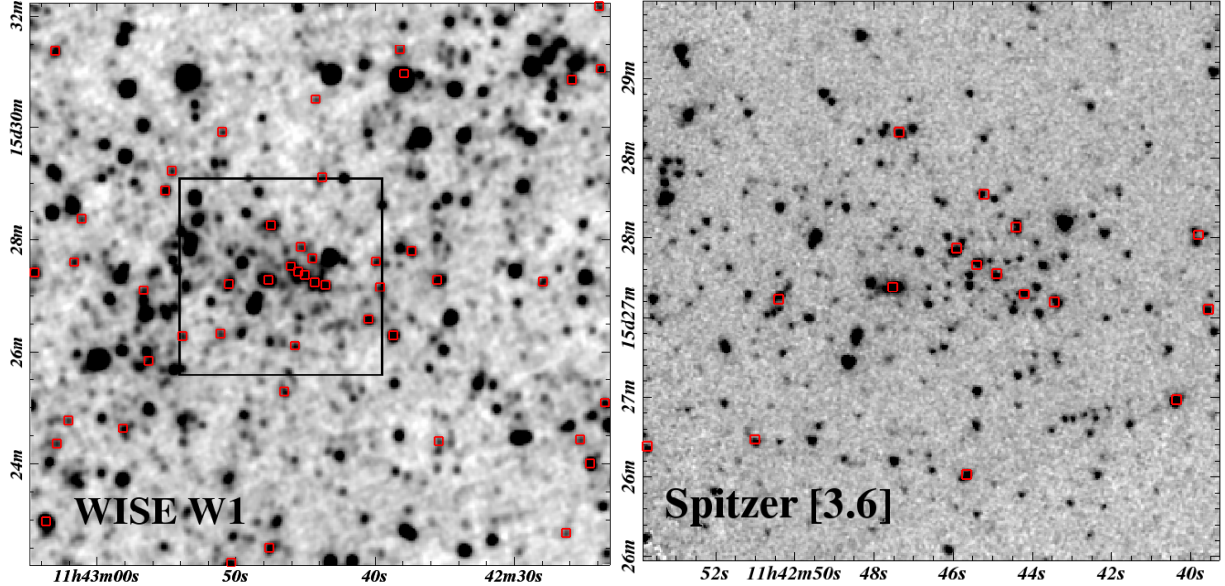


FIG. 1.— The left panel shows the $10' \times 10'$ W1 cutout of MOO J1142+1527 from the AllWISE data release. The black box denotes the $3.5' \times 3.5'$ region centered on the cluster for which we show the corresponding *Spitzer* [3.6] follow-up observation on the right. In both panels the red points denote the locations of individual WISE sources that pass the color, magnitude, and quality cuts as candidate $z \gtrsim 0.75$ galaxies in the MaDCoWS search. In several cases individual WISE sources are resolved into multiple galaxies in the higher resolution *Spitzer*/IRAC images.

high-redshift cluster searches. The first phase of MaDCoWS covered $\sim 10,000 \text{ deg}^2$ within the SDSS footprint; subsequent phases of the program are now extending the search over the full extragalactic sky. In previous papers we presented the first cluster discovered in this survey (Gettings et al. 2012), the redshift distribution of the first 20 clusters ($0.75 < z < 1.3$, Stanford et al. 2014), and Sunyaev-Zel'dovich masses for five clusters (Brodwin et al. 2015). In this paper we present the discovery and confirmation of the most massive cluster yet identified within the MaDCoWS catalog, which is among the ~ 5 most massive clusters expected to exist over the entire sky at $z \gtrsim 1.19$. Throughout the paper we use Vega-based magnitudes and assume a WMAP9 cosmology ($H_0 = 69.7 \text{ km s}^{-1}$, $\Omega_m = 0.2821$, $\Omega_\Lambda = 0.7181$, $\sigma_8 = 0.817$, $n_s = 0.9646$; Hinshaw et al. 2013) unless otherwise specified. For cluster masses and radii we include a c or m subscript to denote whether the values are relative to the critical or mean density.

2. DISCOVERY OF MOO J1142+1527

MaDCoWS is a WISE-based (Wright et al. 2010) search for galaxy clusters at $z \approx 1$ that employs color and magnitude selection to identify massive galaxies at $z \gtrsim 0.75$, and then uses a wavelet technique to detect galaxy overdensities. A key element of this search approach is the combination of the WISE data with uniform optical photometry. The initial detection of Massive Overdense Object (MOO) J1142+1527 used the WISE All-Sky Data Release (Cutri et al. 2012) and SDSS DR8 (Aihara et al. 2011) to identify candidates within the footprint of the SDSS. In this WISE+SDSS MaDCoWS search, MOO J1142+1527 was identified as one of the 200 highest significance cluster candidates.

We have subsequently refined the search algorithm and transitioned to use of the AllWISE Data Release (Cutri et al. 2013). A detailed description of the MaDCoWS survey and detection algorithm will be provided in a forthcoming paper. Briefly, cluster candidates in the current AllWISE+SDSS

search were detected as overdensities of sources with $W1 < 16.9$, $W1 - W2 > 0.2$, and $i_{AB} > 21.3$. MOO J1142+1527 remains the twenty-seventh highest significance candidate in this more recent, refined version of the catalog, with a position $(\alpha, \delta) = (11:42:43.9, 15:27:07)$. In the left panel of Figure 1 we show a WISE [3.6] cutout of the cluster field. The red squares in this panel denote the galaxies that passed the color, magnitude, and quality cuts in this search, highlighting the detected overdensity. Because the WISE magnitude limit and blending of sources in the WISE data result in detection significance being a high scatter richness measure, we have obtained *Spitzer*/IRAC observations to determine more robust richness estimates.

3. SPITZER RICHNESS AND COLOR-MAGNITUDE DIAGRAM

In *Spitzer* Cycle 9 we were awarded 37.9 hours to obtain IRAC $3.6\mu\text{m}$ and $4.5\mu\text{m}$ imaging of the 200 highest significance overdensities from our All-Sky search (Program ID 90177; PI Gonzalez). For each cluster the total exposure times were 180 s in each band, obtained using 30 s frame times and 6 positions in a medium scale cycling dither pattern. This exposure time was designed to reach a nominal 5σ depth of $6 \mu\text{Jy}$ (18.7 mag) at [4.5], which is sufficient to identify galaxies more than one magnitude below L^* up to $z \approx 1.5$.

We reduced and mosaicked the basic calibrated data using the MOPEX package (Makovoz & Khan 2005) and resampled to a pixel scale of $0''.6$. The MOPEX outlier (e.g., cosmic ray, bad pixel) rejection was optimized for the regions of deepest coverage in the center of the maps corresponding to the position of the MaDCoWS detection.

We ran SExtractor (Bertin & Arnouts 1996) in dual image mode for source detection and photometry, using the [4.5] frame as the detection image and adopting IRAC-optimized SExtractor parameters from Lacy et al. (2005). Flux densities were measured in $4''$ diameter apertures. Following Wylezalek et al. (2013), we then applied aperture corrections to the

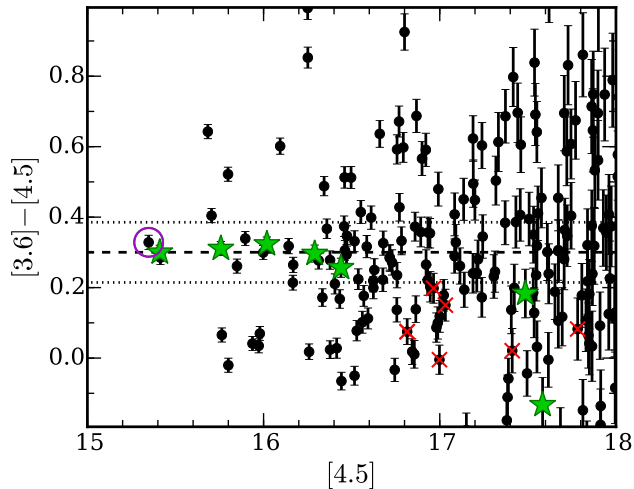


FIG. 2.— The *Spitzer* [3.6] – [4.5] color-magnitude diagram for MOO J1142+1527. The black filled circles represent galaxies that lie within $1'$ of the SZ centroid. Solid green stars denote quality A and B spectroscopic members, while red crosses indicate foreground and background objects listed in Table 1. The open purple circle denotes the galaxy corresponding to the NVSS radio point source (§4). The dashed black line is the expected color from a Bruzual & Charlot (2003) model of a passively evolving, solar metallicity L^* galaxy with a formation redshift $z_f = 3$ at $z = 1.19$; dotted lines indicate the equivalent expected colors for $z = 1.09$ (lower) and $z = 1.29$ (upper).

[3.6] and [4.5] flux densities (factors of 1.42 and 1.45, respectively). We determined a 95% completeness limit of $10 \mu\text{Jy}$, corresponding to limiting magnitude of [4.5] = 18.2. This completeness limit is adopted as the flux density cut in all subsequent analysis. We show the central $3.5' \times 3.5'$ of the IRAC [3.6] image in the right panel of Figure 1. As in the left panel, the red squares denote the positions of *WISE* sources that contributed to detection of the cluster. In some cases, the initial *WISE* source resolves into multiple galaxies with IRAC.

To prioritize follow-up of our Cycle 9 IRAC targets, we defined a simple richness estimator based upon the overdensity of galaxies with red [3.6] – [4.5] color within a fixed angular radius. Specifically, we defined the richness as the number of galaxies with [3.6] – [4.5] > 0.1 within $1'$ of the cluster position measured in the MaDCoWS search. We note that this IRAC color is relatively insensitive to current star formation, selecting both passive and star-forming galaxies in distant clusters. By this measure, MOO J1142+1527 has a richness of 64, which is the ninth highest among the 200 Cycle 9 targets.

Figure 2 shows the *Spitzer* [3.6] – [4.5] color-magnitude diagram for galaxies that lie within $1'$ of the SZ centroid (see §4). These galaxies correspond to the central overdensity of red sources shown in Figure 1. The median color of these galaxies is [3.6] – [4.5] = 0.3, which for a Bruzual & Charlot (2003) passively evolving stellar population corresponds to a galaxy at $z \approx 1.2$. We also highlight the spectroscopically confirmed members (green stars), four of which lie within $1'$ of the SZ centroid, and the non-members (red crosses), which are described in greater detail in the next section.

3.1. Redshift Determination

We used Gemini-North and the W. M. Keck Observatories to obtain spectroscopic confirmation of MOO J1142+1527. Optical pre-imaging for MOO J1142+1527 was obtained with

TABLE 1
SPECTROSCOPIC REDSHIFTS

α	δ	z	Quality	Features
Spectroscopic Members				
11:42:40.04	+15:26:28.1	1.2007	A	H_{β} , [OIII] λ 4959,5007
11:42:40.31	+15:26:28.4	1.20	B	D4000
11:42:42.14	+15:26:59.9	1.19	B	D4000
11:42:43.36	+15:27:05.2	1.19	B	D4000
11:42:43.83	+15:27:01.6	1.179	A	Ca HK, H_{δ}
11:42:45.82	+15:27:25.0	1.19	B	D4000
11:42:49.62	+15:26:59.8	1.1715	B	H_{β} , [OIII] λ 5007
11:42:54.09	+15:26:54.3	1.183	B	H_{β} , [OIII] λ 5007
Foreground/Background Objects				
11:42:41.29	+15:27:59.4	0.7221	A	H_{β} , [OIII] λ 5007
11:42:42.30	+15:26:00.6	0.92	B	D4000
11:42:42.40	+15:26:22.1	1.054	B	Ca HK
11:42:42.69	+15:26:23.5	1.2342	B	[OII] λ 3727
11:42:44.07	+15:27:02.4	1.2401	A	[OIII] λ 4959,5007
11:42:44.94	+15:27:44.7	0.93	B	Ca HK
11:42:45.22	+15:28:07.5	0.93	B	Ca HK

NOTE. — This Table includes all spectroscopic redshifts for objects within $2'$ of the SZ centroid for the cluster.

the Gemini Multi-Object Spectrograph (GMOS) on Gemini-North as part of program GN-2013A-Q-44 (PI Brodwin). We acquired 900 s exposures in the r - and z -bands, sufficient to detect cluster galaxies below L^* at the cluster redshift. Image quality was $0''.68$ for r and $0''.76$ for z . For all spectroscopic programs we designed slit masks using the Gemini rz -band catalogs to identify potential cluster members. We used the red sequence to select the primary targets, weighting by cluster-centric radius, and then filling in the masks with other galaxies at larger radii.

We obtained Gemini GMOS spectroscopy in queue mode on UT 2013 July 02 and UT 2014 March 07, using $1''.0$ slit widths, the R400 grating, and the RG610 filter. Three sets of nod and shuffle sequences were completed at each of two central wavelength settings (8100 and 8200 Å). For each nod and shuffle sequence we used $\pm 0''.75$ nods, with 9 cycles of 60 s exposures, yielding a total on-source exposure time of 6480 s. The seeing ranged between $0''.6$ and $0''.9$ range. We reduced the spectra using standard routines in the Gemini IRAF package.

We subsequently obtained DEIMOS and MOSFIRE spectroscopy at the Keck Observatory on UT 2015 May 12 and UT 2015 June 22, respectively. For DEIMOS, the masks were designed with $1''.1$ width slitlets having a minimum length of $5''$. In addition to the standard target selection criteria, for these masks the *WISE* W1–W2 color was used to prioritize targets at large radii. Observations for two masks were obtained under cloudy conditions with typical seeing of $0''.8$. Four exposures of 1800 s each were obtained on the first mask, and three exposures of 1500 s on the second mask. Both masks used the 600ZD grating with the GG495 filter. We reduced these DEIMOS spectra using the DEEP2 pipeline (Cooper et al. 2012; Newman et al. 2013).

For MOSFIRE, the configurable slit unit was configured for 32 objects, along with five alignment stars. We chose to use the Y bandpass because it covers a spectral range of ~ 9900 to ~ 11200 Å, which encompasses strong rest frame optical emission lines such as [O III] λ 4959,5007 at the probable cluster redshift. The MOSFIRE spectra were obtained using an ABA'B' dither pattern with 120 s exposures and multiple correlated double sampling (MCDS), in the MCDS 16 readout mode. The total integration time was 5760 s. Conditions dur-

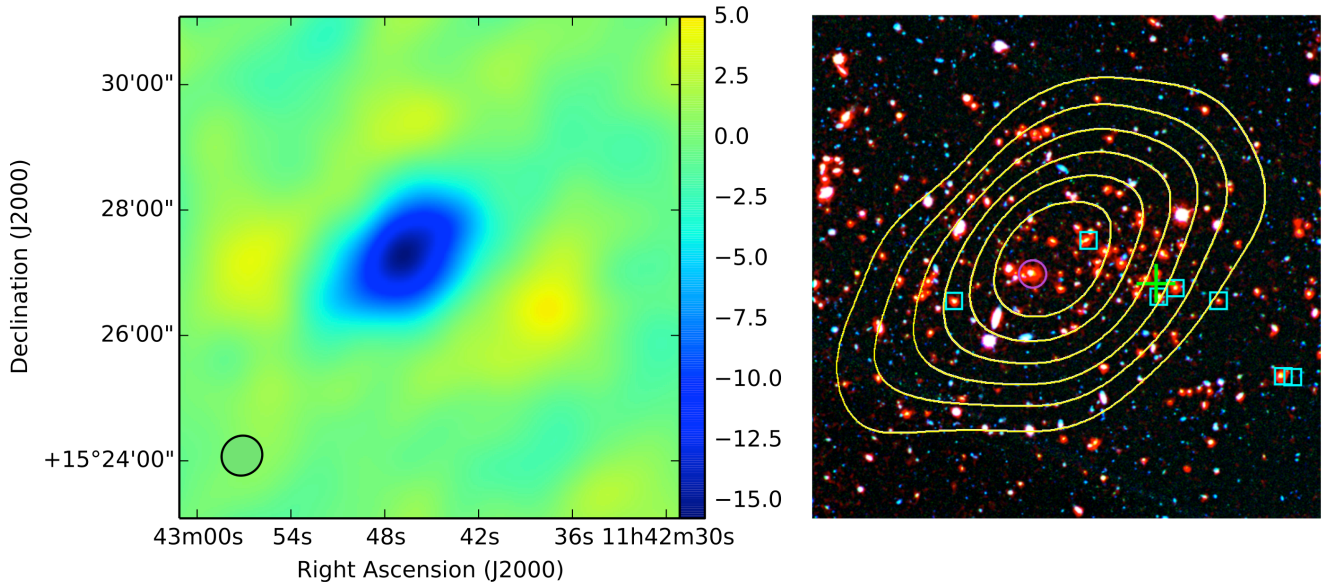


FIG. 3.— Left: CARMA SZ map of the cluster covering an $8' \times 8'$ field, where the scale denotes the significance of the decrement. The black ellipsoid shows the size of the synthesized beam, which has major and minor axes of $39.7''$ and $37.6''$. Right: Composite $r_z[3.6]$ image of MOO J1142+1527, covering the central $3.5' \times 3.5'$, with the SZ contours overlaid. The outer contour corresponds to 3σ , with subsequent contours incrementing by 2σ . The plus sign indicates the original MaDCoWS position, while small squares denote spectroscopic cluster members. The purple circle marks NVSS J114247+152711.

ing the observations were excellent, with seeing measured at $\sim 0''.5$. MOSFIRE spectra were reduced using the standard MOSFIRE data reduction pipeline.¹⁹

The redshift determinations from the combination of Gemini/GMOS, Keck/DEIMOS, and Keck/MOSFIRE spectroscopy are shown in Table 1 for all galaxies that lie within $2'$ (~ 1 Mpc) of the cluster center. We assigned redshifts a quality of A if there are multiple obvious features associated with the same rest frame redshift. Quality B was assigned to redshifts that satisfy one of the following: one and only one emission line is present and is highly likely to be [O II] $\lambda 3727$ given the observed wavelength range of the spectra, an obvious 4000 \AA feature is seen but no other features, or Ca H+K absorption lines are clearly identified. We determined the mean redshift using the Ruel et al. (2014) python implementation of the Beers et al. (1990) biweight estimator. The resulting cluster redshift estimate is $z = 1.188^{+0.002}_{-0.005}$, with the uncertainty derived via bootstrap resampling. The eight galaxies listed as spectroscopic members in Table 1 were those that are retained as members by the redshift estimation code after sigma-clipping.

4. THE SUNYAEV-ZEL'DOVICH DECREMENT AND DERIVED MASS

MOO J1142+1527 was observed with the Combined Array for Research in Millimeter-wave Astronomy (CARMA)²⁰ for approximately 5 hours on-source beginning on UT 2014 July 03. The data are centered around a frequency of 31 GHz. For these observations the array was in its most compact “E+SH” configuration. All 23 antennas were correlated across 2 GHz of bandwidth using the CARMA “spectral line” correlator. To maximize sensitivity to the SZ signal, the “wideband” correlator processed 7.5 GHz of bandwidth for the innermost eight

6.1-meter antennas. CARMA is optimized for the detection of distant clusters via their SZ signatures in this array and correlator configuration. The data from these baselines achieve a sensitivity of 1.2 mJy per $\sim 50'' \times 90''$ beam. The gain calibrator J1224+213 was observed for 3 minutes between 15-minute target observations, and the absolute calibration is derived from Mars via the model of Rudy et al. (1987). Figure 3 (left) shows a CLEAN-deconvolved (Högbom 1974) image of the cluster using all baselines with a Gaussian taper to 10% at $4 k\lambda$, after removal of a point source (see below).

Cluster properties were determined using a Markov Chain Monte Carlo method to simultaneously fit an Arnaud et al. (2010) pressure profile model and point source models to the unflagged data. The single point source in the field, NVSS J114247+152711 (Condon et al. 1998), was located using the higher-resolution, long baseline data from the spectral line correlator. This point source was found to have a flux density of 3.4 mJy, and is coincident with the brightest candidate cluster member (purple circle in Figures 2 & 3), but was not targeted in our spectroscopic program. A second model, consisting of only the point source but no cluster, was also fit to the data. From comparing the goodness of the two fits, the cluster detection significance is 13.2σ . The centroid of the SZ decrement is located at $(\alpha, \delta) = (11:42:46.6, +15:27:15)$, with uncertainties $(\sigma_\alpha, \sigma_\delta) = (4''.4, 3''.0)$. The SZ centroid and *WISE* position, which are separated by $41''$, bracket the peak of the galaxy distribution.

The combined fit of cluster and point source models gives the spherically integrated Comptonization parameter, $Y_{500c} = (9.7 \pm 1.3) \times 10^{-5} \text{ Mpc}^2$. We used the Andersson et al. (2011) M_{500c} - Y_{500c} scaling relation to determine mutually consistent values of M_{500c} and r_{500c} and the associated uncertainties, where $M_{500c} = (4\pi r_{500c}^3/3) \times (500\rho_c)$. This procedure results in a cluster mass and radius of $M_{500c} = (6.0 \pm 0.9) \times 10^{14} M_\odot$ and $r_{500c} = 0.83 \pm 0.04 \text{ Mpc}$, respectively. The quoted uncertainties are derived by combining in quadrature the propa-

¹⁹ <https://keck-datareductionpipelines.github.io/MosfireDRP/>

²⁰ <http://www.mmarray.org>

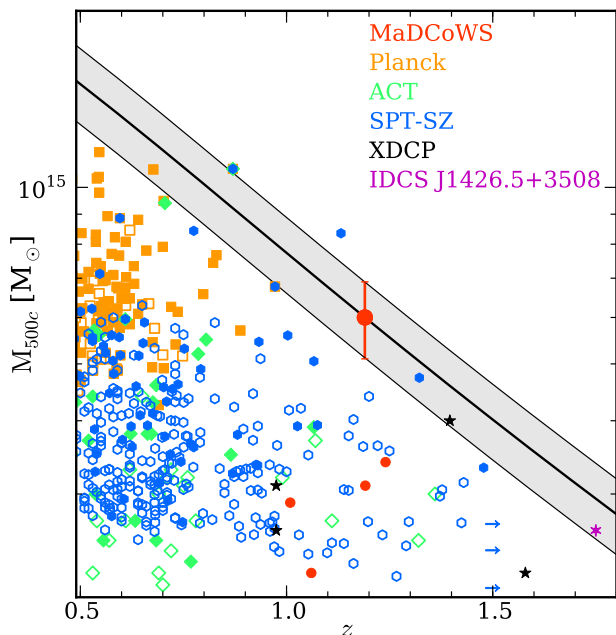


FIG. 4.— Comparison in the mass-redshift plane of MOO J1142+1527 (large red circle with error bars) with other MaDCoWS clusters (red circles, Brodwin et al. 2015), with clusters from the *Planck* (orange squares, Planck Collaboration et al. 2014b), ACT (green diamonds, Marriage et al. 2011; Hasselfield et al. 2013), SPT (blue hexagons, Bleem et al. 2015), and XDCP (black stars, Fassbender et al. 2011) surveys, and with IDCS J1426.5+3508 (purple six-pointed star, Brodwin et al. 2012). We plot the mass from *Planck* for clusters detected in multiple surveys. We use filled symbols for clusters with published spectroscopic redshifts, and open symbols those with photometric redshifts. We make the assumption that *Planck* redshifts are spectroscopic in instances where the type of redshift is unclear. Arrows denote lower limits on SPT photometric redshifts. For XDCP J0044.0-2033 ($z = 1.58$) we plot the updated mass from Tozzi et al. (2015) that uses the Vikhlinin et al. (2009) scaling relation. The black line is a curve of constant comoving number density for a Tinker et al. (2008) mass function; the shaded region indicates the corresponding extension of the 1σ error bars.

gated uncertainty and a 12% intrinsic scatter in M_{500c} at fixed Y_{500c} from Andersson et al. (2011). For the Duffy et al. (2008) mass – concentration relation, the derived mass corresponds to $M_{200c} = (9.9 \pm 1.5) \times 10^{14} M_{\odot}$, or $M_{200m} = (1.1 \pm 0.2) \times 10^{15} M_{\odot}$.

5. DISCUSSION AND SUMMARY

In this paper we have presented confirmation of a massive galaxy cluster at $z = 1.19$. Originally identified by the MaDCoWS project, the cluster MOO J1142+1527 has a mass of $M_{500c} = (6.0 \pm 0.9) \times 10^{14} M_{\odot}$ [$M_{200m} = (1.1 \pm 0.2) \times 10^{15} M_{\odot}$], making it the most massive confirmed galaxy cluster at $z \geq 1.15$ identified by any technique. Figure 4 illustrates the position of this cluster in the mass – redshift plane compared to a selection of recent wide-area cluster surveys. The solid black curve in this Figure is a curve of constant co-moving number density, highlighting that there are few clusters over this entire redshift interval as rare as MOO J1142+1527. The only

more massive cluster known at $z > 1$ is SPT-CL J2106-5844 ($z = 1.13$, $M_{200m} = (1.27 \pm 0.21) \times 10^{15} h_{70}^{-1} M_{\odot}$; Foley et al. 2011). We also include in this Figure IDCS J1426.5+3508 ($z = 1.75$), as it is the closest progenitor analog to MOO J1142+1527 at $z > 1.5$.

The existence of MOO J1142+1527 is not in tension with the Λ CDM paradigm, but such clusters are expected to be extremely rare. We use the halo mass function code *hmf* from Murray et al. (2013)²¹ with a Tinker et al. (2008) mass function to calculate the expected number of such clusters. For WMAP9 and *Planck* (Planck Collaboration et al. 2014a) cosmologies, there are predicted to only be ~ 3 or ~ 7 clusters this massive over the full sky at $z \geq 1.19$, respectively, and only ~ 1 – 2 within our SDSS survey area. The discovery of this cluster highlights the potential of wide area cluster surveys like MaDCoWS to identify such extreme systems, which are natural targets for a range of cosmological and evolutionary investigations. Our ongoing Cycle 11 *Spitzer* program (PID 11080, PI Gonzalez), which targets ~ 1750 additional MaDCoWS candidates drawn from the full extragalactic sky, promises to enable construction of a *sample* of comparably rich galaxy clusters at this epoch.

Support for this research was provided by NASA through *Spitzer* GO program 90177, ADAP grant NNX12AE15G, and NASA Exoplanet Science Institute grants 1461527 and 1486927. The work by SAS at LLNL was performed under the auspices of the U. S. Department of Energy under Contract No. W-7405-ENG-48.

Support for CARMA construction was derived from the Gordon and Betty Moore Foundation; the Kenneth T. and Eileen L. Norris Foundation; the James S. McDonnell Foundation; the Associates of the California Institute of Technology; the University of Chicago; the states of California, Illinois, and Maryland; and the National Science Foundation. CARMA development and operations were supported by NSF under a cooperative agreement and by the CARMA partner universities; the work at Chicago was supported by NSF grant AST-1140019. Additional support was provided by PHY-0114422. This publication makes use of data products from the *Wide-field Infrared Survey Explorer*, a joint project of the University of California, Los Angeles, and the Jet Propulsion Laboratory/California Institute of Technology, funded by NASA. This work is based in part on observations made with the *Spitzer Space Telescope*, which is operated by the Jet Propulsion Laboratory, California Institute of Technology under a contract with NASA. This work is based in part on data obtained at the W. M. Keck and Gemini Observatories. The authors wish to recognize and acknowledge the very significant cultural role and reverence that the summit of Mauna Kea has always had within the indigenous Hawaiian community. We are most fortunate to have the opportunity to conduct observations from this mountain.

Facility: WISE, Spitzer (IRAC), CARMA, Keck:I (MOS-FIRE), Keck:II (DEIMOS) Gemini:Gillett (GMOS)

REFERENCES

Aihara, H., Allende Prieto, C., An, D., et al. 2011, *ApJS*, 193, 29
 Allen, S. W., Evrard, A. E., & Mantz, A. B. 2011, *ARA&A*, 49, 409
 Andersson, K., Benson, B. A., Ade, P. A. R., et al. 2011, *ApJ*, 738, 48
 Arnaud, M., Pratt, G. W., Piffaretti, R., et al. 2010, *A&A*, 517, A92
 Beers, T. C., Flynn, K., & Gebhardt, K. 1990, *AJ*, 100, 32

Bertin, E., & Arnouts, S. 1996, *A&AS*, 117, 393
 Bleem, L. E., Stalder, B., de Haan, T., et al. 2015, *ApJS*, 216, 27
 Bocquet, S., Saro, A., Mohr, J. J., et al. 2015, *ApJ*, 799, 214
 Brodwin, M., Gonzalez, A. H., Stanford, S. A., et al. 2012, *ApJ*, 753, 162
 Brodwin, M., Stanford, S. A., Gonzalez, A. H., et al. 2013, *ApJ*, 779, 138
 Brodwin, M., Greer, C. H., Leitch, E. M., et al. 2015, *ApJ*, 806, 26
 Bruzual, G., & Charlot, S. 2003, *MNRAS*, 344, 1000
 Chen, X. 2010, *Advances in Astronomy*, 2010, arXiv:1002.1416

²¹ See also <https://github.com/steven-murray/hmf>.

- Condon, J. J., Cotton, W. D., Greisen, E. W., et al. 1998, *AJ*, 115, 1693
- Cooper, M. C., Newman, J. A., Davis, M., Finkbeiner, D. P., & Gerke, B. F. 2012, *spec2d: DEEP2 DEIMOS Spectral Pipeline*, Astrophysics Source Code Library, ascl:1203.003
- Cutri, R. M., Wright, E. L., Conrow, T., et al. 2012, <http://wise2.ipac.caltech.edu/docs/release/allsky/expsup/>
- Cutri, R. M., Wright, E. L., Conrow, T., et al. 2013, <http://wise2.ipac.caltech.edu/docs/release/allwise/expsup/>
- Duffy, A. R., Schaye, J., Kay, S. T., & Dalla Vecchia, C. 2008, *MNRAS*, 390, L64
- Ehlert, S., Allen, S. W., Brandt, W. N., et al. 2015, *MNRAS*, 446, 2709
- Eisenhardt, P. R. M., Brodwin, M., Gonzalez, A. H., et al. 2008, *ApJ*, 684, 905
- Fassbender, R., Böhringer, H., Nastasi, A., et al. 2011, *New Journal of Physics*, 13, 125014
- Flaugher, B. 2005, *International Journal of Modern Physics A*, 20, 3121
- Foley, R. J., Andersson, K., Bazin, G., et al. 2011, *ApJ*, 731, 86
- Gettings, D. P., Gonzalez, A. H., Stanford, S. A., et al. 2012, *ApJ*, 759, L23
- Gladders, M. D., & Yee, H. K. C. 2005, *ApJS*, 157, 1
- Hasselfield, M., Hilton, M., Marriage, T. A., et al. 2013, *J. Cosmology Astropart. Phys.*, 7, 8
- Hinshaw, G., Larson, D., Komatsu, E., et al. 2013, *ApJS*, 208, 19
- Högbom, J. A. 1974, *A&AS*, 15, 417
- Lacy, M., Wilson, G., Masci, F., et al. 2005, *ApJS*, 161, 41
- Ma, C.-J., Smail, I., Swinbank, A. M., et al. 2015, *ApJ*, 806, 257
- Makovoz, D., & Khan, I. 2005, in *Astronomical Society of the Pacific Conference Series*, Vol. 347, *Astronomical Data Analysis Software and Systems XIV*, ed. P. Shopbell, M. Britton, & R. Ebert, 81
- Mantz, A. B., Allen, S. W., Morris, R. G., et al. 2014, *MNRAS*, 440, 2077
- Marriage, T. A., Acquaviva, V., Ade, P. A. R., et al. 2011, *ApJ*, 737, 61
- Murray, S. G., Power, C., & Robotham, A. S. G. 2013, *Astronomy and Computing*, 3, 23
- Muzzin, A., Wilson, G., Yee, H. K. C., et al. 2009, *ApJ*, 698, 1934
- Newman, J. A., Cooper, M. C., Davis, M., et al. 2013, *ApJS*, 208, 5
- Planck Collaboration, Ade, P. A. R., Aghanim, N., et al. 2014a, *A&A*, 571, A16
- . 2014b, *A&A*, 571, A29
- Rudy, D. J., Muhleman, D. O., Berge, G. L., Jakosky, B. M., & Christensen, P. R. 1987, *Icarus*, 71, 159
- Ruel, J., Bazin, G., Bayliss, M., et al. 2014, *ApJ*, 792, 45
- Sánchez, E., & DES Collaboration. 2010, *Journal of Physics Conference Series*, 259, 012080
- Sereno, M., Veropalumbo, A., Marulli, F., et al. 2015, *MNRAS*, 449, 4147
- Shandera, S., Mantz, A., Rapetti, D., & Allen, S. W. 2013, *J. Cosmology Astropart. Phys.*, 8, 4
- Stanford, S. A., Gonzalez, A. H., Brodwin, M., et al. 2014, *ApJS*, 213, 25
- Tinker, J., Kravtsov, A. V., Klypin, A., et al. 2008, *ApJ*, 688, 709
- Tozzi, P., Santos, J. S., Jee, M. J., et al. 2015, *ApJ*, 799, 93
- Vikhlinin, A., Kravtsov, A. V., Burenin, R. A., et al. 2009, *ApJ*, 692, 1060
- Williamson, R., Benson, B. A., High, F. W., et al. 2011, *ArXiv e-prints*, arXiv:1101.1290
- Wright, E. L., Eisenhardt, P. R. M., Mainzer, A. K., et al. 2010, *AJ*, 140, 1868
- Wylezalek, D., Galametz, A., Stern, D., et al. 2013, *ApJ*, 769, 79